

Journal of
Mechanics of
Materials and Structures

**EFFECTIVE ELASTIC PROPERTIES OF NANOTUBE REINFORCED
COMPOSITES WITH SLIGHTLY WEAKENED INTERFACES**

Milton Esteva and Pol D. Spanos

Volume 4, N° 5

May 2009



mathematical sciences publishers

EFFECTIVE ELASTIC PROPERTIES OF NANOTUBE REINFORCED COMPOSITES WITH SLIGHTLY WEAKENED INTERFACES

MILTON ESTEVA AND POL D. SPANOS

In this paper a micromechanics approach is presented for determining the effective elastic properties of single-walled carbon nanotube (SWCNT) reinforced composites, while accounting for imperfect bonding in the matrix-inclusion interface. For this purpose, a linear spring layer of vanishing thickness is introduced to represent the interface. Furthermore, the well known Mori–Tanaka (MT) method, in conjunction with the Eshelby’s tensor, is modified to determine the effective elastic properties. The inclusions are considered to be either perfectly aligned infinite long cylinders or aligned ellipsoidal inclusions with a given aspect ratio; cases of perfect alignment or of randomly oriented fibers are treated. The numerical results show that the interface weakening influences the nanocomposite properties significantly only for high values of SWCNT volume fraction. Since most of the currently conducted experiments involve composites which contain small volume fractions, it is thus reasonable based on the findings of this paper to assume perfect bonding for low nanotube volumetric contents.

1. Introduction

Since the discovery of carbon nanotubes [Iijima 1991], single-walled CNTs have attracted increasing scientific interest because of their exceptional mechanical, electrical, and thermal properties. Experimental and theoretical results have shown that the Young’s moduli of SWCNTs are approximately 1 TPa depending on diameter size and chirality [Popov et al. 2000; Yakobson et al. 1996; Pipes et al. 2003; Saether et al. 2003]. Despite these properties, several researchers have reported experiments with modest improvement in the strength and stiffness of polymer nanocomposites (PNC) [Qian et al. 2002; Ajayan et al. 2000]. On the other hand, some others have obtained a substantial increase in the effective properties as shown in Table 1 on the next page. Researchers claim that alignment, dispersion, geometry, and load transfer properties are parameters that could significantly affect the final properties of PNCs [Chen and Tao 2006; Namilae and Chandra 2005].

Several techniques for modeling PNCs have been reported in the open literature. Frankland et al. [2003] have used molecular dynamics (MD) to obtain stress-strain curves of SWCNTs embedded in a polyethylene matrix; the interface has been simulated by nonbonding van der Waals interactions using the Lennard-Jones potential. Odegard et al. [2003] has presented an equivalent-continuum method to obtain an effective continuum fiber that includes interface interaction. Seidel and Lagoudas [2006] have obtained effective continuum fiber properties using a composite cylinder micromechanics approach that can be applied to SWCNT or multiwalled carbon nanotubes (MWCNT). They have used these properties

Keywords: nanocomposites, carbon nanotubes, modeling, imperfect bonding, Mori–Tanaka.

The financial support provided by the Air Force Research Laboratory Clarkson Aerospace Inc. to Rice University is gratefully acknowledged.

Composite	Young's modulus (GPa)	Tensile strength (MPa)	Elongation (%)	NT Orientation
Neat epoxy	$2.02 \pm .078$	83 ± 3.3	6.5 ± 0.17	—
Epoxy + 1 wt.% Bucky Pearl SWNT	$2.12 \pm .093$	80 ± 4.1	5.8 ± 0.33	random
Epoxy + 1 wt.% functionalized	$2.65 \pm .125$	104 ± 3.7	8.5 ± 0.72	random
Epoxy + 4 wt.% functionalized	$3.4 \pm .253$	102 ± 5.4	5.5 ± 0.21	random
TPU	7.7 ± 1	12.4 ± 4.5	852 ± 130	—
TPU + 0.5 wt.% SWNT	14.5 ± 3.4	13.3 ± 4	709 ± 160	aligned

Table 1. Some experimental mechanical properties of polymer nanocomposites. See [Zhu et al. 2004] for the first four rows and [Chen and Tao 2006] for the last two.

with the self consistent (SC), MT and finite element method (FEM) to determine the effective properties for aligned and randomly oriented perfectly bonded inclusions. In that work, an attempt to account for imperfect bonding has been made by using interphase regions involving a multilayer composite cylinder approach requiring the specification of elastic properties and thickness for the interphase layer. Song and Youn [2006] have investigated the effective properties using the asymptotic expansion homogenization method where again perfect interfacial bonding has been assumed. Liu and Chen [2003] have implemented a three dimensional representative volume element (RVE) and have used FEM to obtain effective mechanical properties; in this work perfect bonding between matrix and inclusion has also been assumed. Li and Chou [2003] have adopted a structural mechanics approach to obtain effective properties of cylindrical nanocomposites RVEs in which they have used nonlinear trusses to simulate nonbonding interactions along the interface. Namilae and Chandra [2005] have also discussed the problem of nonperfect bonding. They have developed a multiscale model introducing a constitutive behavior to the interface by means of cohesive zone models. They have used MD to obtain traction-displacement relations and have then implemented them in a numerical scheme using two dimensional axysymmetric FEM and cohesive zone elements for the interface. Despite this sophisticated model, final effective properties strongly depend on RVE dimensions for finite nanotube lengths.

In this paper, a micromechanics model for determining the effective properties of PNCs is presented. The model accounts for imperfect bonding between the matrix and the fiber. For this purpose, a spring layer of finite stiffness but of negligible thickness is introduced in the inclusion model. The layer produces continuous interfacial tractions but discontinuous displacements. The introduction of imperfect interfaces necessitates modified expressions for the Eshelby tensor [1957], which is used in conjunction with the MT method for composites [Qiu and Weng 1990]. In this modified MT approach, the properties of the fiber are derived using a composite cylinder concept [Seidel and Lagoudas 2006]. Results are presented for composites with infinite cylinders and ellipsoidal shape fibers which are either aligned or randomly oriented in the matrix.

2. The original Mori–Tanaka concept

Recently, the original MT approach has been used by several authors to estimate the mechanical properties of nanocomposites [Odegard et al. 2003; Seidel and Lagoudas 2006]. Specifically, interest has

been focused on the calculation of the effective elastic properties of a two phase composite where the inclusion phase is either aligned or randomly oriented. In this section, a review of the derivation of the MT equations is presented first towards accounting for the effect of imperfect bonding between the matrix and the inclusion; obviously this is done towards facilitating the elucidation of the herein adopted procedure, without claiming conceptual novelty.

Assume that the analyzed composite comprises two phases. The matrix is considered to be isotropic and linearly elastic with stiffness tensor \mathbf{L}_0 and volume fraction c_0 . Strictly speaking, the stiffness matrix relates the strains with the stresses they produce by the generalized Hooke's law

$$\sigma_{ij} = L_{ijkl}\varepsilon_{kl}.$$

In a similar way, the inclusion phase is assumed to have ellipsoidal shape and its material is considered to be transversely isotropic with stiffness tensor \mathbf{L}_1 and volume fraction c_1 . Throughout this section explicit tensor notation will be omitted for clarity unless needed.

Consider the two configurations shown in Figure 1. These represent the composite material and the comparison material where the properties of the later are those of the matrix. If displacements are specified at the boundary to produce a uniform strain in both materials (ε_a), the average stress of the composite ($\bar{\sigma}$) and that in the comparison material ($\bar{\sigma}_0$) are $\bar{\sigma} = \mathbf{L}\varepsilon_a$ and $\bar{\sigma}_0 = \mathbf{L}_0\varepsilon_a$, where \mathbf{L} is the effective stiffness tensor of the composite and an overscore represents volume average.

The presence of the inclusions causes the strain field in the matrix to be nonuniform. Thus, the average strain in the matrix is in this case represented by the equation $\bar{\varepsilon}_0 = \varepsilon_a + \bar{\varepsilon}_0^{pt}$. The same change happens to the inclusion phase; the strain is perturbed from that of the matrix and is quantified as

$$\bar{\varepsilon}_1 = \bar{\varepsilon}_0 + \varepsilon_1^{pt}. \quad (1)$$

Using the equivalent inclusion method developed in [Eshelby 1957], a relation between the inhomogeneous inclusion problem (Figure 1, left) and the homogeneous inclusion problem (Figure 1, right) can be pursued. In other words, the properties of the inclusion can be related to the properties of the matrix by the equation

$$\bar{\sigma}_1 = \mathbf{L}_1\bar{\varepsilon}_1 = \mathbf{L}_0(\bar{\varepsilon}_1 - \varepsilon^*), \quad (2)$$

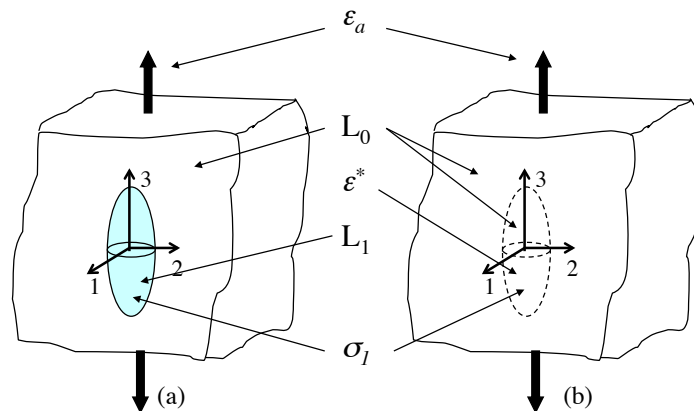


Figure 1. Eshelby's equivalent inclusion problem.

where ε^* is the inclusion eigenstrain. Eshelby [1957] demonstrated that this eigenstrain is related to the inclusion perturbation strain by the equation

$$\varepsilon_1^{pt} = \mathbf{S}\varepsilon^*, \quad (3)$$

where the tensor \mathbf{S} is well known as the Eshelby's tensor; expressions for cylindrical and ellipsoidal inclusions used herein can be found in references such as [Qiu and Weng 1990; Nemat-Nasser and Hori 1998].

Next, solving for ε^* in (2). The expression for the eigenstrain in terms of the average strain in the inclusion is found to be

$$\varepsilon^* = -\mathbf{L}_0^{-1}(\mathbf{L}_1 - \mathbf{L}_0)\bar{\varepsilon}_1. \quad (4)$$

Substituting (4) into (1) and making use of (3), the dilute strain concentration tensor \mathbf{A}^{dil} is found. This tensor relates the average strain in the inclusion with the average strain in the matrix and is given by

$$\bar{\varepsilon}_1 = \mathbf{A}^{\text{dil}}\bar{\varepsilon}_0 = [\mathbf{I} + \mathbf{S}\mathbf{L}_0^{-1}(\mathbf{L}_1 - \mathbf{L}_0)]^{-1}\bar{\varepsilon}_0, \quad (5)$$

where \mathbf{I} is the fourth-order identity tensor.

The relationship between the fiber and matrix strain averages and the overall strain average (ε_a) can be established by the use of the total volume average. That is,

$$c_0\bar{\varepsilon}_0 + c_1\bar{\varepsilon}_1 = \varepsilon_a. \quad (6)$$

By substituting (5) into (6), the strain concentration tensor of the matrix (\mathbf{A}_0) is obtained. This quantity relates the applied strain with the average strain in the matrix by the equation

$$\bar{\varepsilon}_0 = \mathbf{A}_0\varepsilon_a = [c_0\mathbf{I} + c_1\mathbf{A}^{\text{dil}}]^{-1}\varepsilon_a. \quad (7)$$

To derive the expression for the effective elastic moduli, the key assumption in the MT method is introduced. That is, when identical particles are introduced in the composite, the average strain in the inclusion is related to the average strain in the matrix by the dilute strain concentration tensor

$$\bar{\varepsilon}_1 = \mathbf{A}^{\text{dil}}\bar{\varepsilon}_0. \quad (8)$$

This means, that to account for inclusion interaction, the applied strain that each inclusion feels is the average strain in the matrix. Substituting (7) into (8), the nondilute strain concentration tensor is obtained (\mathbf{A}^{ndil}). This tensor relates the applied strain to the average strain in the inclusion by the equation

$$\bar{\varepsilon}_1 = \mathbf{A}^{\text{ndil}}\varepsilon_a = \mathbf{A}^{\text{dil}}\mathbf{A}_0\varepsilon_a. \quad (9)$$

Finally, to find the overall effective stiffness tensor for aligned inclusions, a similar expression as in (6) is used but for the case of stresses this is

$$\bar{\sigma} = c_0\bar{\sigma}_0 + c_1\bar{\sigma}_1 = \mathbf{L}\varepsilon_a, \quad (10)$$

where substitution of Hooke's law in (10) gives

$$\bar{\sigma} = c_0\mathbf{L}_0\bar{\varepsilon}_0 + c_1\mathbf{L}_1\bar{\varepsilon}_1 = \mathbf{L}\varepsilon_a.$$

Solving for L and using (7) and (9), the final expression for the effective stiffness tensor of the MT estimate is obtained as

$$\mathbf{L} = (c_0 \mathbf{L}_0 + c_1 \mathbf{L}_1 \mathbf{A}^{\text{dil}})(c_0 \mathbf{I} + c_1 \mathbf{A}^{\text{dil}})^{-1}. \quad (11)$$

This is the equation to implement the MT method for an aligned two phase composite.

It is also of interest to derive a MT estimate when the inclusions are randomly oriented inside the matrix. To this aim, the effective composite stiffness tensor will be determined using the orientational average of the pertinent properties. The difference between the aligned and the randomly oriented inclusions lies in that for the latter case the relation (6) becomes

$$c_0 \bar{\varepsilon}_0 + c_1 \{\mathbf{A}^{\text{dil}} \bar{\varepsilon}_0\} = (c_0 \mathbf{I} + c_1 \{\mathbf{A}^{\text{dil}}\}) \bar{\varepsilon}_0 = \varepsilon_a, \quad (12)$$

where the brackets $\{\cdot\}$ designate the average over all possible orientations [Qiu and Weng 1990]. Similarly, (10) becomes

$$\bar{\sigma} = c_0 \mathbf{L}_0 \bar{\varepsilon}_0 + c_1 \{\mathbf{L}_1 \bar{\varepsilon}_1\} = (c_0 \mathbf{L}_0 + c_1 \{\mathbf{L}_1 \mathbf{A}^{\text{dil}}\}) \bar{\varepsilon}_0 = \mathbf{L} \varepsilon_a. \quad (13)$$

Finally, combining (12) and (13), the expression for the MT estimate for the case of randomly oriented inclusions is obtained as

$$\mathbf{L} = (c_0 \mathbf{L}_0 + c_1 \{\mathbf{L}_1 \mathbf{A}^{\text{dil}}\})(c_0 \mathbf{I} + c_1 \{\mathbf{A}^{\text{dil}}\})^{-1}, \quad (14)$$

which is similar to the expression for the case of aligned inclusions, except for those appropriate averaged quantities. Clearly, the MT approach can be used as a tool for deriving an effective stiffness tensor for the composite material. Specific studies regarding the MT method have been previously presented [Qiu and Weng 1990; Tucker and Liang 1999; Schjødt-Thomsen and Pyrz 2001; Benveniste 1987; Wang and Pyrz 2004].

3. Mori–Tanaka approach for composites with slightly weakened interfaces

In a model developed by Qu [1993] in conjunction with generic composite materials mechanics, imperfection in the interface can be introduced by using a layer of insignificant thickness in which tractions remain continuous and displacements become discontinuous. The equations that model the interfacial traction continuity and the displacement jump (Δu_i) at the interface can be written as

$$\Delta \sigma_{ij} n_j \equiv [\sigma_{ij}(S^+) - \sigma_{ij}(S^-)] n_j = 0, \quad (15)$$

and

$$\Delta u_i \equiv [u_i(S^+) - u_i(S^-)] = \eta_{ij} \sigma_{jk} n_k \quad (16)$$

respectively. In (15) and (16), S and n represent the interface and its unit outward normal vector, respectively. The terms $u(S^+)$ and $u(S^-)$ are the values of the displacements when approaching from outside and inside of the inclusion respectively. The second order tensor, η_{ij} , accounts for the compliance of the spring layer. It is obvious that when the tensor η_{ij} tends to zero (infinite stiffness), the displacement jump is zero and continuity in displacements are recovered. This tensor is chosen to be symmetric and positive definite and can be expressed in the form

$$\eta_{ij} = \alpha \delta_{ij} + (\beta - \alpha) n_i n_j, \quad (17)$$

where n_i is the normal outward vector and δ_{ij} is the Kronecker delta.

It is important to address the physical meaning of the parameters α and β . To define these terms more completely, an example is presented. Consider a two dimensional plane where a horizontal surface divides the matrix and the inclusion material (see Figure 2). The unit outward normal vector n is pointing in the vertical direction. Performing summation over dummy indexes in (16), the displacement jumps in direction 1 and 2 are

$$\begin{aligned} \Delta u_1 &= \eta_{11}\sigma_{11}n_1 + \eta_{11}\sigma_{12}n_2 + \eta_{12}\sigma_{21}n_1 + \eta_{12}\sigma_{22}n_2, \\ \Delta u_2 &= \eta_{21}\sigma_{11}n_1 + \eta_{21}\sigma_{12}n_2 + \eta_{22}\sigma_{21}n_1 + \eta_{22}\sigma_{22}n_2. \end{aligned} \tag{18}$$

Because the outward normal vector is in the vertical direction, $n_1 = 0$ and $n_2 = 1$. Using these values, (18) reduces to

$$\Delta u_1 = \eta_{11}\sigma_{12}n_2 + \eta_{12}\sigma_{22}n_2, \quad \Delta u_2 = \eta_{21}\sigma_{12}n_2 + \eta_{22}\sigma_{22}n_2. \tag{19}$$

In a similar manner and also making use of the Kronecker delta properties, (17) is used to generate the four required elements in (19). That is,

$$\begin{aligned} \eta_{11} &= \alpha\delta_{11} + (\beta - \alpha)n_1n_1 = \alpha, & \eta_{12} &= \alpha\delta_{12} + (\beta - \alpha)n_1n_2 = 0, \\ \eta_{21} &= \alpha\delta_{21} + (\beta - \alpha)n_2n_1 = 0, & \eta_{22} &= \alpha\delta_{22} + (\beta - \alpha)n_2n_2 = \beta. \end{aligned} \tag{20}$$

Substituting (20) into (19), the displacement jumps in direction 1 and 2 are

$$\Delta u_1 = \alpha\sigma_{12} = \alpha\tau, \quad \Delta u_2 = \beta\sigma_{22} = \beta\sigma. \tag{21}$$

It is clear in (21) that α and β are parameters that represent the compliance in the tangential and normal directions respectively as shown in Figure 2. Furthermore, setting the parameter β to zero (infinite stiffness in the normal direction) prevents material interpenetration.

After introducing the imperfect interface into the equivalent inclusion method, Qu found a modified expression for the Eshelby’s tensor, for the case of ellipsoidal inclusions with slightly weakened interfaces. The new expression is written as

$$\bar{S}_{ijkl}^M = S_{ijkl} + (L_{ijpq} - S_{ijpq})H_{pqrs}L_{rsmn}(I_{mnkl} - S_{mnkl}), \tag{22}$$

where S_{ijkl} is the original Eshelby’s tensor and L_{ijkl} is the matrix stiffness tensor. The second term in the right hand side of (22) is produced due to the introduction of the weakened interface, where the tensor

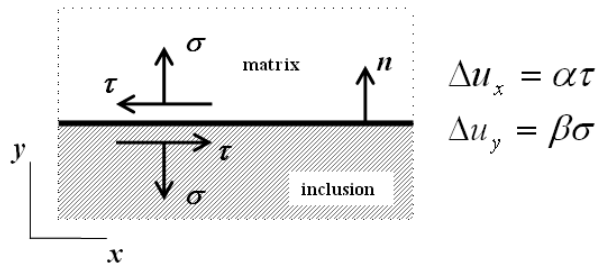


Figure 2. Physical meaning of parameters α and β in the compliance tensor η_{ij} .

\mathbf{H} is given by the equation

$$H_{ijkl} = \alpha P_{ijkl} + (\beta - \alpha) Q_{ijkl};$$

expressions for tensor \mathbf{P} and \mathbf{Q} are given in the Appendix.

Once the modified Eshelby's tensor has been included in the analysis, the modified MT estimate is introduced. Following the same procedure to find (11) and using the result in [Qu 1993] for the average strains, the expression for the modified MT estimate for a two phase aligned composite is obtained as

$$\mathbf{L} = (c_o \mathbf{L}_o + c_1 \mathbf{L}_1 \mathbf{A}^{\text{dil}}) (c_o \mathbf{I} + c_1 [\mathbf{A}^{\text{dil}} + \mathbf{H} \mathbf{L}_1 \mathbf{A}^{\text{dil}}])^{-1}, \quad (23)$$

where

$$\mathbf{A}^{\text{dil}} = [\mathbf{I} + \bar{\mathbf{S}}^M \mathbf{L}_0^{-1} (\mathbf{L}_1 - \mathbf{L}_0)]^{-1}. \quad (24)$$

In all this new expressions, if the parameters α and β are set to zero, the tensor \mathbf{H} vanishes and equations (22), (23), and (24) reduce to the original MT expression shown in (11). It is worth mentioning that the expression for the effective elastic properties in (23) is length dependent, in contrast to the original MT which is aspect ratio dependent.

When the inclusions are randomly oriented inside the matrix, determination of the effective elastic properties can be obtained following the same procedure as in (14). Using the result found in [Qu 1993] for the total average strain, the MT expression with slightly weakened interfaces for the case of randomly oriented inclusions is

$$\mathbf{L} = (c_o \mathbf{L}_0 + c_1 \{\mathbf{L}_1 \mathbf{A}^{\text{dil}}\}) (c_o \mathbf{I} + c_1 \{\mathbf{A}^{\text{dil}}\} + c_1 \{\mathbf{H} \mathbf{L}_1 \mathbf{A}^{\text{dil}}\})^{-1}. \quad (25)$$

Likewise, if the parameters α and β are set to zero, the tensor \mathbf{H} vanishes and (25) reduce to the original MT expression shown in (14). Similar studies have been reported for the case of inclusions with specific shape and material properties [Benveniste and Aboudi 1984; Benveniste 1985; Hashin 1991].

4. Implementation of the Mori–Tanaka estimate

As stated in the previous sections, to obtain effective elastic properties by means of the MT method it is necessary to use fourth-order tensor operations. To avoid the complexity that this task involves, the notation originally developed in [Walpole 1981] and used later in [Qiu and Weng 1990; Wang and Pyrz 2004] will be used. In this notation, a general symmetric fourth-order tensor can be represented by the equation

$$\mathbf{L} = (2k, l, l', n, 2m, 2p), \quad (26)$$

where the quantities k, l, l', n, m and p are related to the fourth-order tensor elements by the equation

$$k = \frac{1}{2}(L_{2222} + L_{2233}), \quad l = L_{1122}, \quad l' = L_{2211}, \quad n = L_{1111}, \quad m = \frac{1}{2}(L_{2222} - L_{2233}), \quad p = L_{1212},$$

in which for the case of a transversely isotropic stiffness tensor, the quantities l and l' are identical. An isotropic stiffness tensor can also be represented using this notation and the aforementioned quantities are defined as

$$k = K + \frac{1}{3}\mu, \quad l = l' = K - \frac{2}{3}\mu, \quad n = K + \frac{4}{3}\mu, \quad m = p = \mu, \quad (27)$$

where K and μ are the bulk modulus and the shear modulus, respectively. Thus, whenever a fourth-order tensor is expressed using this notation, algebraic operations of this kind of tensor can be easily performed.

The expression for the MT estimate requires the use of tensor inner products. The computation of the inner product of the two tensors $\mathbf{A} = (c, g, h, d, e, f)$ and $\mathbf{B} = (c', g', h', d', e', f')$ is given by the equation

$$\mathbf{AB} = (cc' + 2hg', gc' + dg', hd' + ch', dd' + 2gh', ee', ff'). \quad (28)$$

Besides inner products, tensor inversion is also required by the MT estimate. The inverse operation of tensor \mathbf{A} , denoted by \mathbf{A}^{-1} , satisfies the equation

$$\mathbf{AA}^{-1} = \mathbf{I}, \quad (29)$$

where \mathbf{I} is the identity tensor. If this tensor is expressed as $\mathbf{I} = (1, 0, 0, 1, 1, 1)$, it follows from (28) and (29) that

$$\mathbf{A}^{-1} = \left(\frac{d}{cd - 2gh}, -\frac{g}{cd - 2gh}, -\frac{h}{cd - 2gh}, \frac{c}{cd - 2gh}, \frac{1}{e}, \frac{1}{f} \right).$$

As shown in (14), when the inclusions in the composite are randomly oriented within the matrix, certain quantities require to be averaged over all possible directions. The result of this operation is a naturally isotropic tensor. Only two properties are required to fully define the tensor. For the case of tensor \mathbf{L} in (26), the isotropic bulk and shear modulus are calculated as

$$K = \frac{1}{9}[4k + 2(l + l') + n], \quad \mu = \frac{1}{15}[k - (l + l') + n + 6(m + p)].$$

Once these two quantities are obtained, one can form the new isotropic tensor by using the expressions in (27).

5. Estimation of nanocomposite effective elastic properties

The modified MT method is applied herein to obtain the effective elastic properties of the composite. Fiber and matrix material properties (for all cases in this paper) are identical to those shown in Table 2.

The work done in [Namilae and Chandra 2005] was used to obtain reasonable values for the parameter α , they used molecular dynamics to perform a fiber pull out test. Three values for the parameter α are chosen for all cases in this section (0, 0.01, and 0.05 nm/GPa) and β is set to zero to prevent material interpenetration. In this section, computations of composites with aligned inclusions and those with randomly oriented fibers are presented.

Matrix: EPON 862	
$E = 2.026$	$\nu = 0.3$
Effective carbon nanotubes	
$E_{11} = 704$ GPa	$\nu_{12} = 0.14$
$E_{22} = 345$ GPa	$\nu_{23} = 0.37$
$\mu_{12} = 227$ GPa	$\phi = 1.7$ nm

Table 2. Input data for effective properties computations. From [Seidel and Lagoudas 2006].

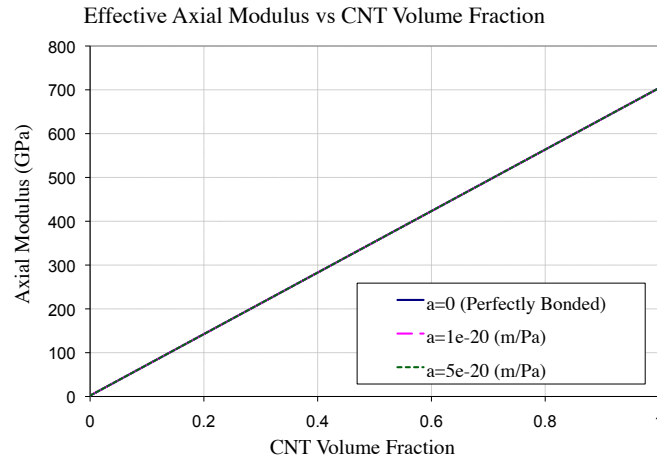


Figure 3. Effective axial modulus for composites with cylindrical inclusions.

Aligned SWCNT composites. It is known that for the case of isotropic matrices and aligned transversely isotropic inclusions, the resulting overall properties are also transversely isotropic. Five independent elastic properties fully describe the behavior of this type of materials. The modified MT method is applied and the computations assume aligned infinitely long nanotubes. The results shown in Figure 3 are for the effective axial modulus. No effect of weakened interfaces is observed as expected and the behavior is that of the rule of mixtures.

Figure 4 shows how interface properties impact the transverse modulus; it is slightly affected for almost the entire range of volume fractions but it is significantly reduced for values greater than 0.8. For the axial and transverse shear moduli similar behavior is found (see Figure 5). An important result of introducing imperfect interfaces in the model is that composite properties do not converge to nanotube

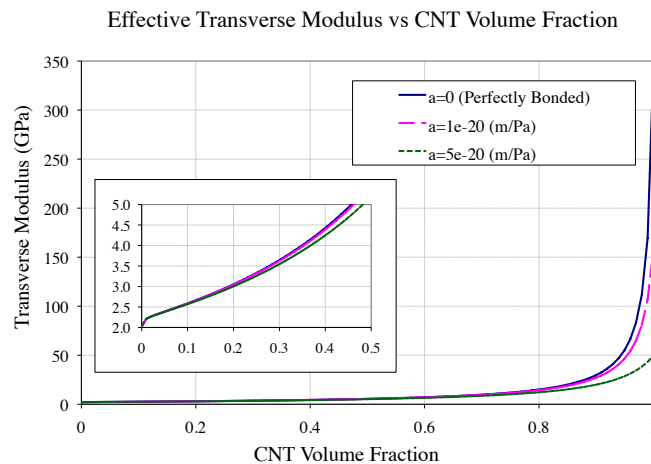


Figure 4. Dependence of transverse modulus on parameter α for composites with cylindrical inclusions, $d = 1.7$ nm.

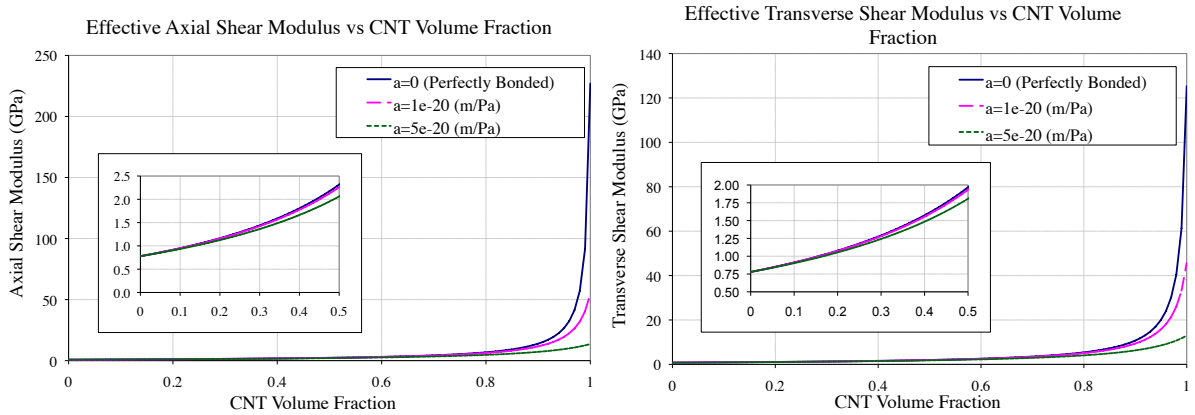


Figure 5. Effective axial (left) and transversal (right) shear moduli versus parameter α for composites with cylindrical inclusions, $d = 1.7$ nm.

properties when the volume fraction approaches 1, as can be seen in Figure 4 and Figure 5. This can be expected as the fiber material is no longer homogeneous; it is affected by the presence of the negligible layer with displacement discontinuities.

Another important aspect of the effective nanocomposite properties computation is to study the impact of inclusion aspect ratio (length/diameter) when the fibers are not considered infinitely long. Calculations of this type of composite can be conducted using the modified Eshelby’s tensor for ellipsoidal inclusions. Expressions for the computation of required tensors are shown in the Appendix, in which numerical integration is used due to the complex terms generated. Figure 6 captures the impact of the parameter α on the calculation of the axial and transverse effective modulus. These results are for the specific case of a nanotube diameter of 1.7 nm and an aspect ratio of 50. Similarly to the case of infinitely long nanotubes, the transverse modulus is affected more than the axial modulus by the presence of imperfect

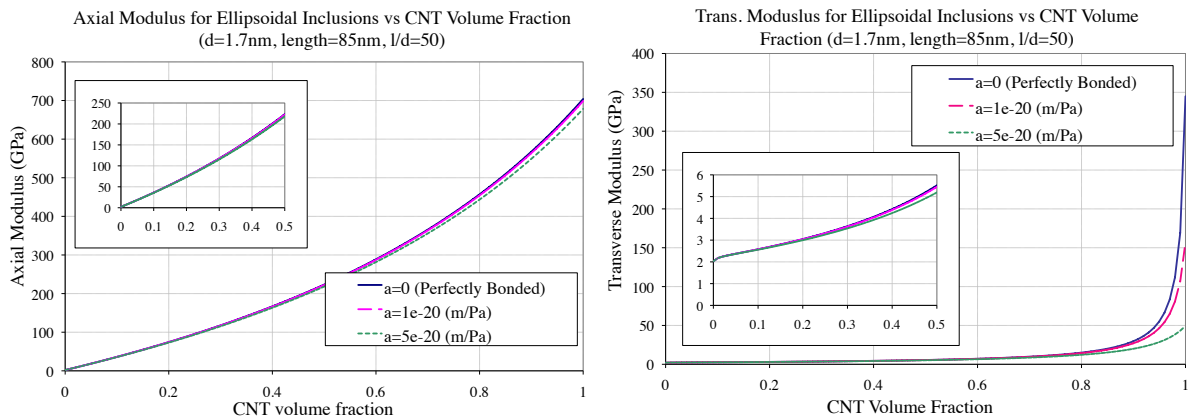


Figure 6. Effective axial (left) and transverse (right) moduli versus parameter α for composites with ellipsoidal inclusions, $d = 1.7$ nm, length=85 nm.

bonding. And, in this case, aspect ratio starts to slightly affect the axial modulus as it does not follow the rule of mixtures anymore.

Randomly oriented SWCNT composites. Next, the properties of SWCNT composites with randomly oriented cylindrical and ellipsoidal fibers are calculated assuming nanotubes have good dispersion in the matrix. The final elastic properties for both types of inclusions are fully isotropic because they are obtained from an average over all possible orientations [Qiu and Weng 1990]. Figure 7 shows the effective modulus of randomly oriented infinitely long cylinders and ellipsoids respectively. They both have the same type of behavior, but the effective properties predicted for the ellipsoidal inclusions are less than those for the cylindrical inclusions due to the aspect ratio dependence. The impact of introducing imperfect bonding is still more evident for high volume fractions (more than 0.6) as noted in Figure 7. Finally, Figure 8 provides the result on the effect of aspect ratio and volume fraction in the effective properties of nanocomposites with ellipsoidal randomly oriented inclusions and slightly weakened interfaces ($\alpha = 0.05 \text{ nm/GPa}$). As expected, for high values of aspect ratio (more than 200) the behavior of cylindrical inclusions is reached but for values less than 200, effective modulus is highly affected.

6. Concluding remarks

The effect of introducing imperfect bonding in the calculation of PNC effective properties has been studied in this paper. Effective properties have been computed using a modified MT method to include the effect of the weakened interface. The properties of the effective fiber have been obtained by a composite cylinder method [Seidel and Lagoudas 2006]. Furthermore, three different configurations for the fibers have been considered. First, nanotubes were treated as aligned infinitely long cylinders where bonding imperfection affects only the transverse properties of the composite for high volume fractions values. Second, the nanotubes were treated as ellipsoidal fibers with a given aspect ratio. In this case, both the axial and the transverse properties were affected by the aspect ratio. Once more, the weakened interface became important only for high volume fraction values. Lastly, the cylindrical and the ellipsoidal fibers

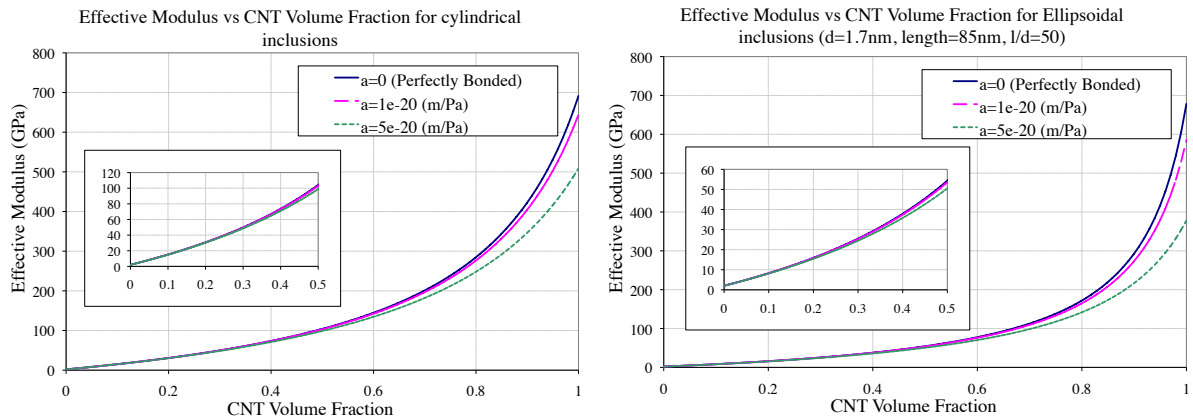


Figure 7. Effective modulus dependence on parameter α for composites with either cylindrical (a) or ellipsoidal (b) randomly oriented inclusions.

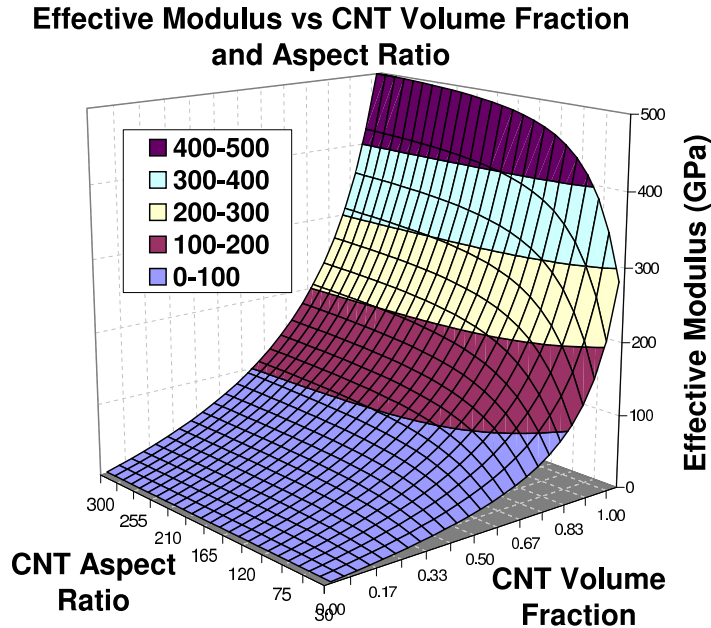


Figure 8. Effective modulus versus CNT volume fraction and aspect ratio for ellipsoidal inclusions with $\alpha = 0.05$ nm/GPa.

were treated as randomly oriented fibers. For the cylindrical fibers, the effective properties did not follow the rule of mixtures as in the aligned case, and the weakened interface became significant only at high volume fractions.

All of the numerical results reported have shown that interfacial weakening influences the effective nanocomposite properties significantly for high values of SWCNT volume fractions. Since most of the currently conducted experiments involve composites which contain small volume fractions, it is reasonable to assume perfect bonding for low nanotube volumetric contents. Nonetheless, the developed procedure is applicable for assessing the interfacial weakening effect for an arbitrary volume fraction.

The H tensor

The tensor H needed to compute the modified MT estimate can be written as follows with axis 1 as the symmetry axis

$$H_{ijkl} = \alpha P_{ijkl} + (\beta - \alpha) Q_{ijkl},$$

where the components of tensors P and Q depend on the inclusion shape and can be obtained using the following expressions:

For ellipsoids

$$P_{ijkl} = \frac{3}{16\pi} \int_0^\pi \left[\int_0^{2\pi} (\delta_{ik} \hat{n}_j \hat{n}_l + \delta_{jk} \hat{n}_i \hat{n}_l + \delta_{il} \hat{n}_k \hat{n}_j + \delta_{jl} \hat{n}_k \hat{n}_i) n^{-1} d\theta \right] \sin \phi d\phi,$$

$$Q_{ijkl} = \frac{3}{4\pi} \int_0^\pi \left[\int_0^{2\pi} \hat{n}_i \hat{n}_j \hat{n}_k \hat{n}_l n^{-3} d\theta \right] \sin \phi d\phi, \quad n = \sqrt{\hat{n}_i \hat{n}_i},$$

$$\hat{n} = \left(\frac{\cos \phi}{a_1}, \frac{\sin \phi \cos \theta}{a_2}, \frac{\sin \phi \sin \theta}{a_3} \right)^T.$$

For cylinders ($a_2 = a_3 = a$ and $a_1 \rightarrow \infty$) so

$$P_{2222} = P_{3333} = 4P_{3131} = 4P_{2121} = 2P_{2323} = \frac{3\pi}{8a},$$

$$Q_{2222} = Q_{3333} = 3Q_{2233} = 3Q_{3322} = 3Q_{2323} = \frac{9\pi}{32a},$$

with all others being 0.

References

- [Ajayan et al. 2000] P. M. Ajayan, L. S. Schadler, C. Giannaris, and A. Rubio, "Single-walled carbon nanotube-polymer composites: strength and weakness", *Adv. Mater.* **12**:10 (2000), 750–753.
- [Benveniste 1985] Y. Benveniste, "The effective mechanical behaviour of composite materials with imperfect contact between the constituents", *Mech. Mater.* **4**:2 (1985), 197–208.
- [Benveniste 1987] Y. Benveniste, "A new approach to the application of Mori–Tanaka's theory in composite materials", *Mech. Mater.* **6**:2 (1987), 147–157.
- [Benveniste and Aboudi 1984] Y. Benveniste and J. Aboudi, "A continuum model for fiber reinforced materials with debonding", *Int. J. Solids Struct.* **20**:11–12 (1984), 935–951.
- [Chen and Tao 2006] W. Chen and X. Tao, "Production and characterization of polymer nanocomposite with aligned single wall carbon nanotubes", *Appl. Surf. Sci.* **252**:10 (2006), 3547–3552.
- [Eshelby 1957] J. D. Eshelby, "The determination of the elastic field of an ellipsoidal inclusion, and related problems", *Proc. R. Soc. Lond. A* **241**:1226 (1957), 376–396.
- [Frankland et al. 2003] S. J. V. Frankland, V. M. Harik, G. M. Odegard, D. W. Brenner, and T. S. Gates, "The stress-strain behavior of polymer-nanotube composites from molecular dynamics simulation", *Compos. Sci. Technol.* **63**:11 (2003), 1655–1661.
- [Hashin 1991] Z. Hashin, "Thermoelastic properties of particulate composites with imperfect interface", *J. Mech. Phys. Solids* **39**:6 (1991), 745–762.
- [Iijima 1991] S. Iijima, "Helical microtubules of graphitic carbon", *Nature* **354** (1991), 56–58.
- [Li and Chou 2003] C. Li and T.-W. Chou, "Multiscale modeling of carbon nanotube reinforced polymer composites", *J. Nanosci. Nanotechnol.* **3**:5 (2003), 423–430.
- [Liu and Chen 2003] Y. J. Liu and X. L. Chen, "Evaluations of the effective material properties of carbon nanotube-based composites using a nanoscale representative volume element", *Mech. Mater.* **35**:1–2 (2003), 69–81.
- [Namilaie and Chandra 2005] S. Namilaie and N. Chandra, "Multiscale model to study the effect of interfaces in carbon nanotube-based composites", *J. Eng. Mater. Technol. (ASME)* **127**:2 (2005), 222–232.
- [Nemat-Nasser and Hori 1998] S. Nemat-Nasser and M. Hori, *Micromechanics: overall properties of heterogeneous materials*, 2nd rev. ed., North Holland, Amsterdam, 1998.

- [Odegard et al. 2003] G. M. Odegard, T. S. Gates, K. E. Wise, C. Park, and E. J. Siochi, "Constitutive modeling of nanotube-reinforced polymer composites", *Compos. Sci. Technol.* **63**:11 (2003), 1671–1687.
- [Pipes et al. 2003] R. B. Pipes, S. J. V. Frankland, P. Hubert, and E. Saether, "Self-consistent properties of carbon nanotubes and hexagonal arrays as composite reinforcements", *Compos. Sci. Technol.* **63**:10 (2003), 1349–1358.
- [Popov et al. 2000] V. N. Popov, V. E. Van Doren, and M. Balkanski, "Elastic properties of crystals of single-walled carbon nanotubes", *Solid State Comm.* **114**:7 (2000), 395–399.
- [Qian et al. 2002] D. Qian, G. J. Wagner, W. K. Liu, M.-F. Yu, and R. S. Ruoff, "Mechanics of carbon nanotubes", *Appl. Mech. Rev. (ASME)* **55**:6 (2002), 495–533.
- [Qiu and Weng 1990] Y. P. Qiu and G. J. Weng, "On the application of Mori–Tanaka's theory involving transversely isotropic spheroidal inclusions", *Int. J. Eng. Sci.* **28**:11 (1990), 1121–1137.
- [Qu 1993] J. Qu, "The effect of slightly weakened interfaces on the overall elastic properties of composite materials", *Mech. Mater.* **14**:4 (1993), 269–281.
- [Saether et al. 2003] E. Saether, S. J. V. Frankland, and R. B. Pipes, "Transverse mechanical properties of single-walled carbon nanotube crystals, I: Determination of elastic moduli", *Compos. Sci. Technol.* **63**:11 (2003), 1543–1550.
- [Schjødt-Thomsen and Pyrz 2001] J. Schjødt-Thomsen and R. Pyrz, "The Mori–Tanaka stiffness tensor: diagonal symmetry, complex fibre orientations and non-dilute volume fractions", *Mech. Mater.* **33**:10 (2001), 531–544.
- [Seidel and Lagoudas 2006] G. D. Seidel and D. C. Lagoudas, "Micromechanical analysis of the effective elastic properties of carbon nanotube reinforced composites", *Mech. Mater.* **38**:8–10 (2006), 884–907.
- [Song and Youn 2006] Y. S. Song and J. R. Youn, "Modeling of effective elastic properties for polymer based carbon nanotube composites", *Polymer* **47**:5 (2006), 1741–1748.
- [Tucker and Liang 1999] C. L. Tucker, III and E. Liang, "Stiffness predictions for unidirectional short-fiber composites: review and evaluation", *Compos. Sci. Technol.* **59**:5 (1999), 655–671.
- [Walpole 1981] L. J. Walpole, "Elastic behavior of composite materials: theoretical foundations", *Adv. Appl. Mech.* **21** (1981), 169–242.
- [Wang and Pyrz 2004] J. Wang and R. Pyrz, "Prediction of the overall moduli of layered silicate-reinforced nanocomposites, I: Basic theory and formulas", *Compos. Sci. Technol.* **64**:7–8 (2004), 925–934.
- [Yakobson et al. 1996] B. I. Yakobson, C. J. Brabec, and J. Bernholc, "Nanomechanics of carbon tubes: instabilities beyond linear response", *Phys. Rev. Lett.* **76**:14 (1996), 2511–2514.
- [Zhu et al. 2004] J. Zhu, H. Peng, F. Rodriguez-Macias, J. L. Margrave, V. N. Khabashesku, A. M. Imam, K. Lozano, and E. V. Barrera, "Reinforcing epoxy polymer composites through covalent integration of functionalized nanotubes", *Adv. Funct. Mater.* **14**:7 (2004), 643–648.

Received 17 Apr 2008. Revised 16 May 2009. Accepted 17 May 2009.

MILTON ESTEVA: mesteva@rice.edu

Rice University, Department of Mechanical Engineering and Material Science - MS 321, PO Box 1892, Houston, TX 77521-1892, United States

POL D. SPANOS: spanos@rice.edu

Rice University, Department of Mechanical Engineering and Material Science - MS 321, PO Box 1892, Houston, TX 77521-1892, United States